

FORMATION METROLOGY AND CONTROL FOR LARGE SEPARATED OPTICS SPACE TELESCOPES*

Edward METTLER, William G. BRECKENRIDGE, and Marco B. QUADRELLI

Jet Propulsion Laboratory
California Institute of Technology
Pasadena, CA 91109

Abstract - In this paper we present formation flying performance analysis initial results for a representative large space telescope composed of separated optical elements [Mett 02]. A *virtual-structure* construct (an equivalent rigid body) is created by unique metrology and control that combines both centralized and decentralized methods. The formation may be in orbit at GEO for super-resolution Earth observation, as in the case of Figure 1, or it may be in an Earth-trailing orbit for astrophysics, Figure 2. Extended applications are envisioned for exo-solar planet interferometric imaging by a formation of very large separated optics telescopes, Figure 3. Space telescopes, with such large apertures and $f/10$ to $f/100$ optics, are not feasible if connected by massive metering structures. Instead, the new virtual-structure paradigm of information and control connectivity between the formation elements provides the necessary spatial rigidity and alignment precision for the telescope.

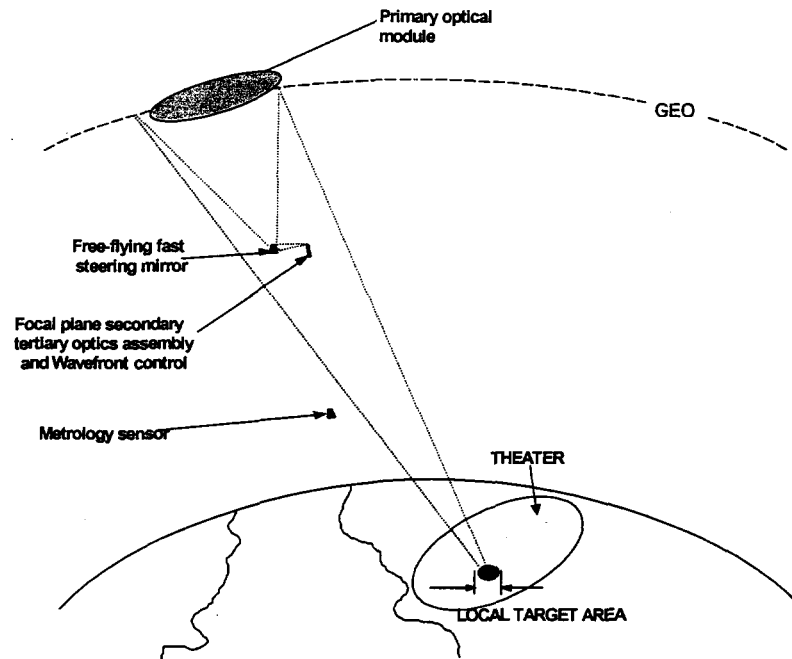


Fig. 1: GEOTEL Imaging a Target on Earth (not to scale)

* October 29-31 2002 International Symposium on Formation Flying: Missions and Technologies, Toulouse, France

† This research was performed at the Jet Propulsion Laboratory, Caltech, under contract with NASA.

1 – INTRODUCTION

The formation flying performance analysis initial results for a representative large space telescope composed of separated optical elements is presented in this paper. The geostationary telescope (GEOTEL) is a 25-meter $f/10$ aperture telescope [Mett 02], Fig.1 and 2, that is composed of 6 bodies: A 25-m Primary Mirror Membrane (PMM), Free Flying Relay Mirror (FFM), Focal Plane Assembly (FPA with a Fast Steering Mirror (FSM) and secondary/tertiary stages), Primary Figure Sensor (PFS), Scanning Electron Beam (SEB) for PMM shape control, and an Orbiting Sunshade (OSS). The reflective optics telescope represents a gossamer concept that can have many variations, extending to very large diffractive glass membrane spinning primaries (Fig. 3). Our goal was to assess the feasibility of implementing a large space telescope by maneuvering and station-keeping the separated optics to the required geometry and precision that obviates the need for a massive connective metering structure.

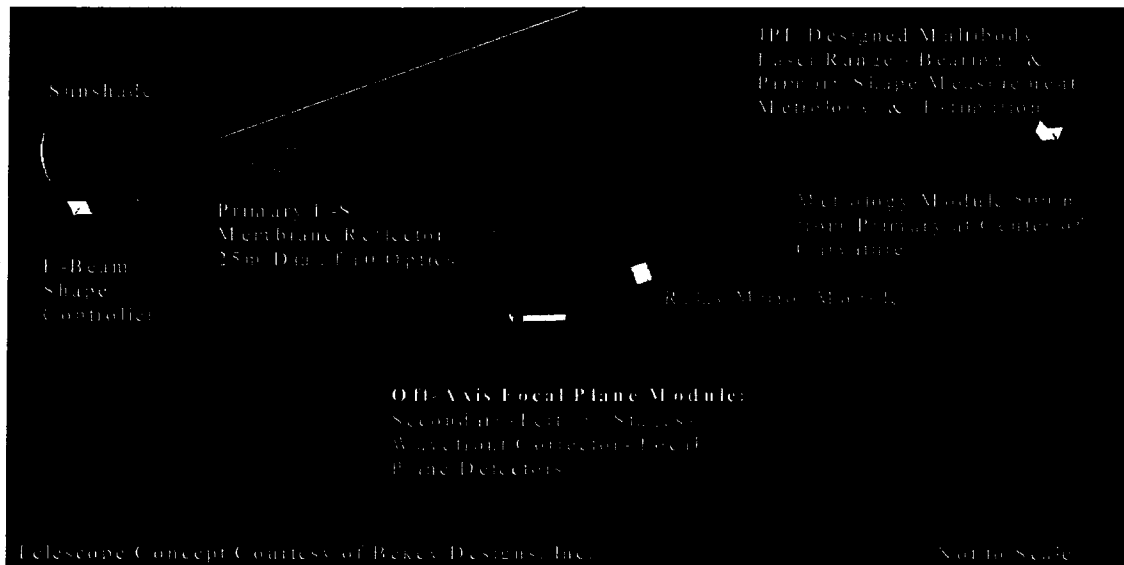


Figure 2: Formation Flying Virtual Structure Space Telescope

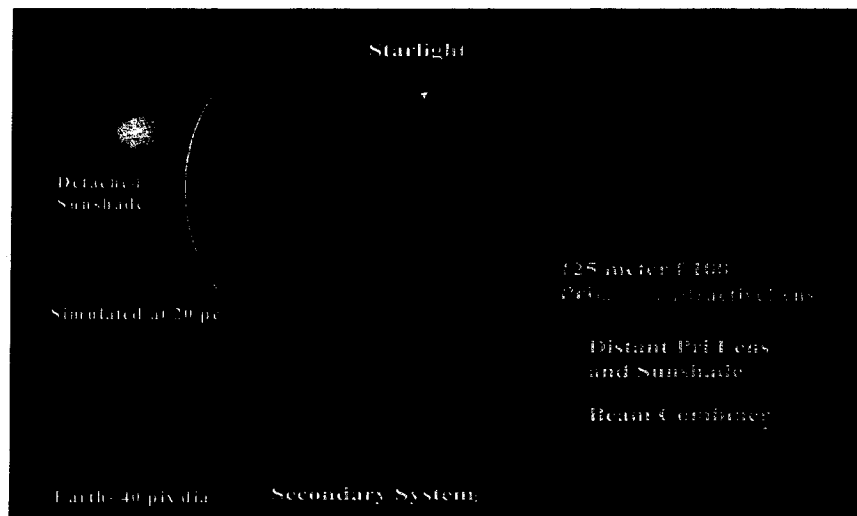


Figure 3. Diffractive Optics Concept for Exo-Solar System Planet Imaging

2 - FORMATION CONTROL ARCHITECTURE

In the GEOTEL metrology of Figure 4, a distributed sensing and control architecture enables a **virtual-truss** 3D rigidity of the separated telescope elements and maintains the tight tolerances on overall planarity and alignments of the optical system. Relative measurements between linear neighbors and an off-axis observer are depicted. Range, range rate, azimuth and elevation data are obtained and processed both locally on each body and globally by a 'Commander' function. The **challenges** in formation sensing and control are: 1) The 25-meter, $f/10$, PMM and its necessary optical path alignments place severe constraints on multi-body metrology and station-keeping knowledge (nanometer range and sub-microradian bearing) of individual measurements, and sub-mm real-time motion control); 2) Diffraction limited imaging requires fine placement of the target image in the entrance aperture of the FPA to enable focal plane image stabilization and wave-front correction; and 3) The need for coordinated multi-body acquisition and line-of-sight pointing maneuvers motivates real-time formation control using an onboard analytical model of the telescope optics, with Centralized and Decentralized sensing, estimation, and control authority [Mett 02].

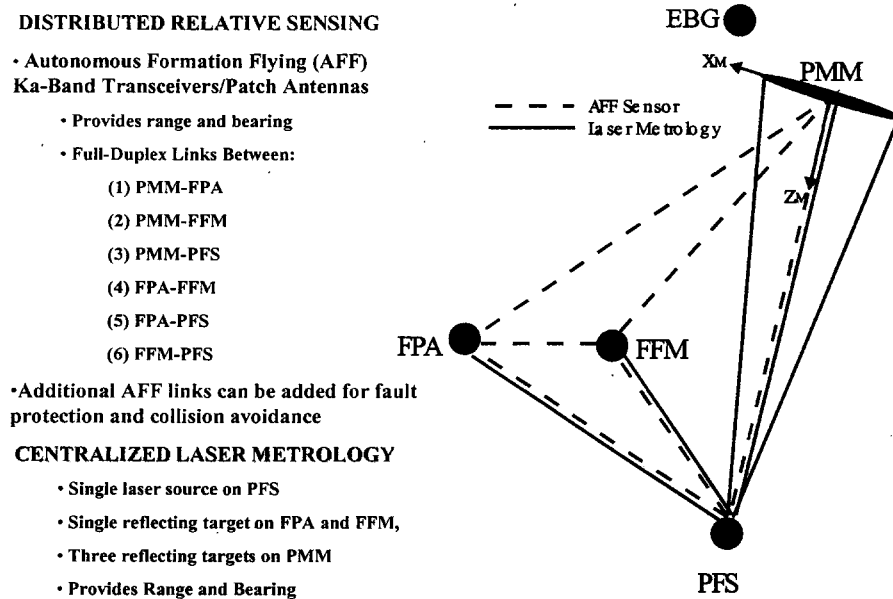


Figure 4: GEOTEL Metrology

The operational **assumptions and constraints** for the system include: deployment and acquisition such that all elements are at their nominal orbital positions, accurate to within a meter. The PMM is station-kept so that its CG follows a geostationary orbit, and the CG of the PMM is located at its mechanical center. The optical system is assumed to have been calibrated, using a ground beacon reference in concert with ray path mapping, resulting in on-board optical models that are accurate enough to predict the principle ray direction and target image location. The OSS is both attitude and orbit controlled to provide shade of the PMM over the entire year. All elements of the formation station-keep with respect to the PMM. Relative position knowledge is provided by an RF-coarse and Optical-fine metrology system. Absolute orbit position and attitude is provided by a Global Differential GPS, and Inertial Measurement subsystems on each element.

Configuring the telescope is done by **predictive open loop** acquisition to place the target image within the entrance aperture of the FPA with an accuracy that enables an image-sensed FPA centering and stabilization stage to function; followed by **closed loop** focal plane image sensed correction of offsets, and image stabilization. Motion control of all separated elements is by FEEP

(field emission electrostatic propulsion) micro-thrusters (with optional small reaction wheels). Target Image **acquisition** accuracy allocations for centering within the FPA entrance aperture are ± 10 mm per axis lateral (2 dof) and ± 10 mm on-axis, for depth of field. Further sub-allocations in Image Location include both knowledge and control errors combined on an RSS basis are: FPA Image Location Error (3.54 mm); FFM Image Location Error (3.54 mm); Optical Model Image location Error (8.66 mm). The **closed-Loop** FPA image-sensed stabilization control must provide < 500 microns lateral centering and on-axis errors in order to be within the dynamic range of a Liquid Crystal Wavefront Corrector. It must also provide image stabilization for near diffraction-limited resolution, and sensing of "excessive offset" for the predictive mode acquisition control.

The Telescope axis is defined as the line perpendicular to the ring of the Primary Mirror and is pointed in the desired inertial direction by attitude control of the Primary (2 dof). The PMM surface is controlled to be spherical with specified radius of curvature (500m) and center of curvature on the telescope axis. The PMM **shape** is measured by the PFS at the desired center of curvature and aligned with the Primary. The shape **actuator** is the E-Beam that station-keeps and aligns with respect to the Primary at an on-axis point behind the Primary (e.g. 50m). The E-Beam will irradiate the primary's electrostatic membrane mirror to correct shape errors at a one second refresh rate. PFS data is sent to the **Optical Model** that determines the required focal point with respect to the Primary (3 position and 2 attitude dof). For any Theater, the PMM and FPA remain stationary and the FFM moves around in the 3.5-m square theater image (500km at the surface) to intercept various individual target images (17.5mm square, 2.5km at the surface). This is shown in Fig. 6.

3 - FORMATION DYNAMICS & CONTROL

The formation's most active elements are 5 free-flying modules (sunshade dynamics are neglected). The free-flyers are: S0-the PMM, S1-the FFM, S2-the FPA, S3-the PFS, and S4-the SEB. With S_0 at the origin of the coordinate frame the relative coordinates of S_i , $i=1, \dots, 4$ are:

S_1	$p_1 = 40$	$q_1 = 0$	$r_1 = 235.7753$
S_2	$p_2 = 50$	$q_2 = 0$	$r_2 = 240$
S_3	$p_3 = 0$	$q_3 = 0$	$r_3 = 500$
S_4	$p_4 = 50$	$q_4 = 0$	$r_4 = -50$

Table 1. GEOTEL Coordinates, meters

Where (p_i, q_i, r_i) are the formation coordinates of the S_i . The coordinates above define a virtual formation that is to be maintained throughout the flight. The orbit is circular. The formation **dynamics** is determined (and numerically integrated) with respect to the Orbiting Reference Frame. The motion of the system is described with respect to a local vertical-local horizontal (LV-LH) orbiting reference frame of origin O_{ORF} that rotates with mean motion and orbital radius. A general type of orbit can be accommodated in the model, as the orbital geometry at the initial time is defined in terms of its six orbital elements, and the orbital dynamics equation for point O_{ORF} is propagated forward in time under the influence of the gravitational field of the primary Earth for LEO, and the Sun for deep space with Earth as a third body perturbation effect. Refer to [Mett 02] for detailed equations of system kinematics, translational and rotational dynamics, and control laws. The translation and rotation **control** method for the individual elements is a trajectory-shaped proportional, derivative, and acceleration feed-forward algorithm that smoothly transitions and converges during a formation re-targeting slew to precision station-keeping for target imaging.

4 - FORMATION RF METROLOGY

The Autonomous Formation Flying (AFF) RF metrology on each element receives range and phase data, at each of 3 antennae, from Ka-band signals output by transceivers. There are 6 one-way links for each element pair (Figure 4). The 6 links provide an **RF truss** to determine the relative position and attitude of the two elements. Assuming that all the common errors in the system have been calibrated, and attitudes are known accurately from Attitude Estimation, each **truss** can be viewed as an independent measurement of the relative position of the two elements. Previous analysis has shown that the measurement accuracy can be characterized by independent range (along the LOS) and bearing (2 dof pointing normal to the LOS) errors.

The assumptions of the sensor model are as follows. First, the attitude estimate accuracy is small with respect to required bearing accuracy. Second, calibrated parameters are available for the alignment between AFF antennas and attitude sensors, the AFF clock differences, and the AFF phase difference biases. Observations are 6 ranges and 4 phase differences. The phase differences enhance bearing accuracy but not range. The accuracy of an estimate from one set of AFF measurements is approximately $v_{\text{range}} = v_r / 6$ and $v_{\text{bearing}} = v_{\text{ph}} * 2 / (d_i^2 + d_j^2)$ per axis, for the measurement from body-*i* to body-*j*, where *d* is a metric of the AFF receiver array size [meters], and v_r is the variance of range measurements from the ranging code correlation $\approx (1\text{cm})^2$, v_{ph} is the variance of phase measurements from carrier correlation $(10\mu\text{m})^2$.

5 - FORMATION OPTICAL METROLOGY

The formation optical metrology is a new system that enables determination of range and bearing of all elements, and the figure of the Primary Mirror (Figure 5). This underlying **vector metrology** is based on the following three components: (1) **Array Heterodyne Interferometer (AHI)**. The AHI is a heterodyne interferometer that simultaneously measures relative range of multiple targets on a surface and enables multi-target high precision linear and angular metrology. The target surface is illuminated with a beam of light that is reflected and then interfered with a reference wavefront. The resulting interference pattern is detected with a CCD or an APS (Active Pixel Sensor) array. Because it is a heterodyne interferometer, i.e., target and reference beams are shifted in frequency relative to each other by a heterodyne frequency, each detector pixel produces an AC output oscillating at the heterodyne frequency. The phase of this oscillation, relative to a reference oscillator or another pixel, is proportional to the relative range. (2) **Modulation Sideband Technology for Absolute Ranging (MSTAR)**. MSTAR enables unambiguous range determination for moving targets. The MSTAR sensor is an upgrade to the AHI that turns it into a range sensor with a long ambiguity range, while retaining high precision (**nanometer**) of a heterodyne interferometer. It is a two-color interferometer implemented with a *single frequency* stable laser, a key consideration for long-range metrology. Measurements at two wavelengths are simultaneous, enabling measurements of non-stationary targets. Two wavelengths are generated and isolated by a combination of high-speed phase modulators and frequency shifters. No high-speed signals need to be detected, providing simple signal processing and high sensitivity. (3) **Boresight Pointing Sensor (BPS)**. The BPS allows enables high-precision (**sub-microradian**) angular metrology without high-precision pointing optics. The addition of MSTAR and BPS to the AHI turns the AHI from a static figure sensor into a dynamic formation vector metrology sensor. A vector metrology sensor configuration is shown in Figures 2, 5. The returning light from the Primary Mirror and retro-reflective targets mounted on the target elements is imaged on the APS. The phases of heterodyne modulations at each corresponding pixel on the APS are processed to give range, and the image centroids are calculated on the chip to give the bearing angle of the target corresponding to a given spot. These innovations enable us to combine PMM **figure sensing** and formation **vector metrology** into a single package on the PFS [Mett 02].

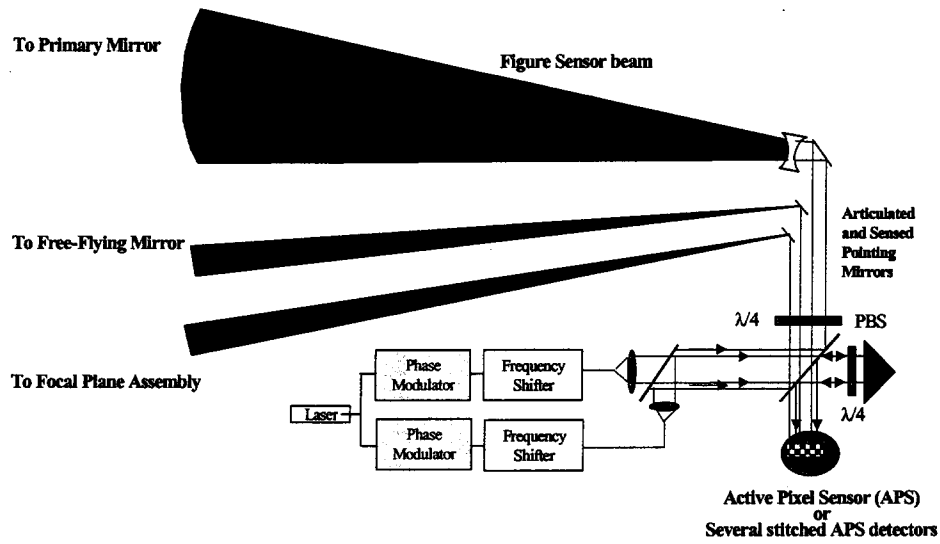


Figure 5. GEOTEL Vector Metrology Sensor

6 - FORMATION ESTIMATOR

For simplification of this discussion, we will deal with the relative translation estimator based only on the AFF radio-frequency metrology (Figure 4). The translation estimator estimates only the relative position and velocity of adjacent spacecraft. This implies that the measurements used depend only on relative position and are not correlated to other system variables. The metrology measurements are also assumed to be independent and uncorrelated between measurements. After measurement and estimation, the following input data is available to the Commander/Controller of the formation: For each module, we have linear position, velocity, acceleration vectors, quaternion, angular velocity, angular acceleration vectors in relative bearing and bearing rate, relative range and range rate, all measured with respect to the vehicle's body frame, the neighbor spacecraft body frame, and the inertial frame. The estimation of the attitude of each module is decentralized. Star tracker and gyro measurements on each element are processed to give the module's attitude relative to an inertial frame. Accelerometer data and relative position measurements from an AFF are also available. The AFF measurement covariance matrix, \mathbf{R} , is characterized by range and bearing (2 dof) estimate uncertainties and has its principal axes aligned with the measurement vector. Let the vector $\mathbf{v} = r\mathbf{u}$ where r is the range and \mathbf{u} is the unit vector along the LOS, v_r the variance of range estimate $= \sigma_r^2$, and v_b the variance of bearing estimate, per axis $= \sigma_b^2$. Then the measurement covariance matrix is $\mathbf{R} = v_r \mathbf{u}\mathbf{u}^T + v_b r^2(1 - \mathbf{u}\mathbf{u}^T)$. A random vector from the population represented by \mathbf{R} can be generated from independent, zero mean, unit variance random numbers, w_i , by $\mu_{\text{error}} = \sigma_r \mathbf{u} w_1 + (1 - \mathbf{u}\mathbf{u}^T) w_2$. The estimator structure is as follows:

$$\begin{aligned} \mathbf{r} &= \mathbf{y} - \mathbf{H}\mathbf{x} \\ \mathbf{K} &= \mathbf{X}\mathbf{H}^T(\mathbf{H}\mathbf{X}\mathbf{H}^T + \mathbf{R})^{-1} \\ \mathbf{x}_+ &= \mathbf{x} + \mathbf{K}\mathbf{r} \\ \mathbf{X}_+ &= (\mathbf{I} - \mathbf{K}\mathbf{H})\mathbf{X}(\mathbf{I} - \mathbf{K}\mathbf{H})^T + \mathbf{K}\mathbf{R}\mathbf{K}^T \end{aligned}$$

Where \mathbf{r} is the measurement residual, \mathbf{K} is the extended Kalman filter gain, \mathbf{X} is the estimator state covariance, \mathbf{x} the estimator state, and the subscripts $+$ ($-$) denote the state before or after update. Optical metrology measurements can be treated in the same way as the RF metrology described above, and combined to give even higher precision state estimates.

7 - FORMATION COMMANDER

The formation of telescope elements is considered as a single “rigid body” with a telescope Line-of-Sight fixed in “body” coordinates. That coordinate system is defined co-linear with the PMM coordinate system. All elements have fixed locations with respect to the Primary Mirror except the Free Flying Mirror that is at its mean position. The desired formation attitude places the body-fixed LOS in the inertial direction of the desired Target. The formation configuration with the FPA offset from the PMM axis is used to keep the telescope LOS away from the formation elements to avoid obscuration and stray light. The FFM is intended to intercept a target image from the PMM and precisely redirect it into the entrance aperture of the Focal Plane Assembly. To accomplish this, two conditions must be met at the FFM position. The first one is that FFM must be on the line from the PMM to the Image. The second one is that the PMM-FFM-FPA path length must equal the focal length of the telescope. A solution puts the FFM on an ellipsoid, with foci at the FPA and PMM, at the intersection with the PMM-Image line. Alternatively, the FFM is at the intersection of the PMM-Image line and the plane bisecting the FPA-Image line segment shown in Figure 6-left. The mirror normal is oriented to bisect the lines to the FPA and PMM. For moderate changes in target location within a field around the aim-point, the FFM can be moved to intercept image points as shown in Figure 6-right. Refer to [Mett 02] for the entire Formation Commander architecture.

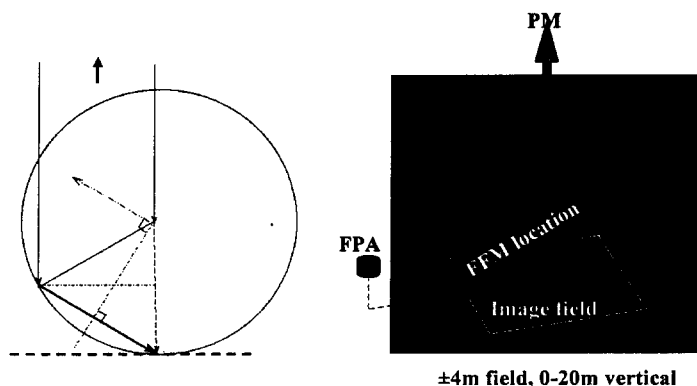


Fig. 6: Free-flying Mirror Commander

8 - NUMERICAL SIMULATIONS

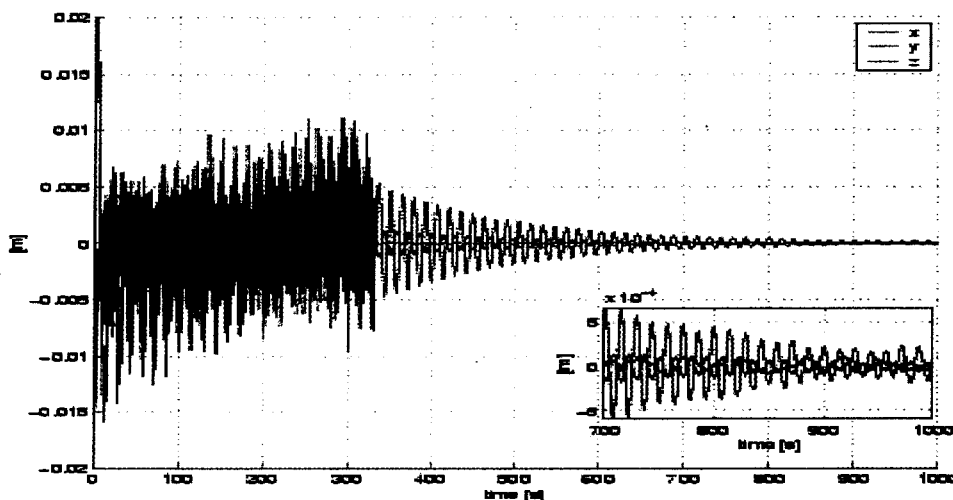


Fig. 7: FFM Position Errors (meters) vs. Time for 1 degree Retargeting in the Orbital Plane.

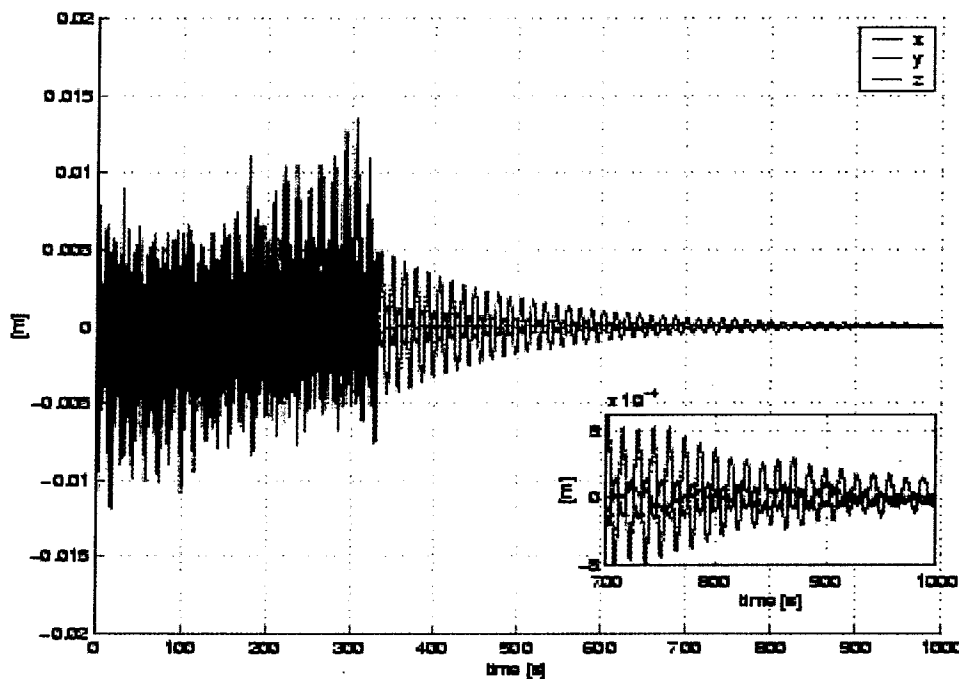


Fig. 8: FPA Position Error (meters) vs Time for a 1 Degree Retargeting

9 – CONCLUSIONS

In this paper we have presented initial feasibility analysis results (Fig. 7, 8) for formation flying a representative space telescope composed of separated optics [Mett 02]. Such concepts are envisioned for astrophysics and Earth observation. Preliminary formation station-keeping and target image placement precision, using proportional FEEP micro-thrusters and combined RF and Optical Vector Metrology, is 200 to 300 microns, and several microradians orientation. This will both center the target image in the FPA and be within the desired 500 microns dynamic range of the wavefront corrector in the FPA. The impact of Formation Flying large aperture lightweight telescopes will be revolutionary, and make possible first-order scientific breakthroughs.

10 – ACKNOWLEDGEMENTS

The research of the authors was carried out at the Jet Propulsion Laboratory, California Institute of Technology, under a contract with the National Aeronautic and Space Administration. We gratefully acknowledge the contributions of our colleagues Drs. David S. Bayard and Serge Dubovitsky. We also wish to thank our JPL sponsor Dr. Fred Y. Hadaegh for his valued advice and support. Our sincere appreciation also goes to Dr. Ivan Bekey, President of Bekey Designs, Inc., and Dr. Richard Baron of JPL for their fundamental large aperture telescope concepts.

REFERENCES:

- [Mett 02] E. Mettler, W. Breckenridge, M. Quadrelli: *Dynamics and Control of a 25-meter Aperture Virtual Structure Gossamer Telescope in GEO*, AIAA-2002-4435, AIAA/AAS Astrodynamics Conference, Monterey, CA, 08-07-02.